

# Landau theory of crystal plasticity

R. Baggio,<sup>1,2</sup> E. Arbib,<sup>3</sup> P. Biscari,<sup>3</sup> S. Conti,<sup>4</sup> L. Truskinovsky,<sup>2</sup> G. Zanzotto,<sup>5</sup> and O.U. Salman<sup>1,\*</sup>

<sup>1</sup>CNRS, LSPM, Université Paris 13, France

<sup>2</sup>PMMH, ESPCI, Paris, France

<sup>3</sup>Department of Physics, Politecnico di Milano, Italy

<sup>4</sup>Institut für Angewandte Mathematik, Universität Bonn, Germany

<sup>5</sup>DPG, Università di Padova, Italy

(Dated: 23 avril 2019)

We show that nonlinear continuum elasticity can be effective in modeling plastic flows in crystals if it is viewed as Landau theory with an infinite number of equivalent energy wells whose configuration is dictated by the symmetry group  $GL(3, \mathbb{Z})$ . Quasi-static loading can be then handled by athermal dynamics, while lattice based discretization can play the role of regularization. As a proof of principle we study in this Letter dislocation nucleation in a homogeneously sheared 2D crystal and show that the global tensorial invariance of the elastic energy foments the development of complexity in the configuration of collectively nucleating defects. A crucial role in this process is played by the unstable higher symmetry crystallographic phases, traditionally thought to be unrelated to plastic flow in lower symmetry lattices.

Crystal plasticity is the simplest among yield phenomena in solids [1], and yet it has been compared in complexity to fluid turbulence [2, 3]. The intrinsic irregularity of plastic flow in crystals [4] is due to short and long range interaction of crystal defects (dislocations) [5] dragged by the applied loading through a rugged energy landscape [6–8]. Fundamental understanding of plastic flow in crystals is crucial for improving hardening properties of materials [9], extending their fatigue life [10], controlling their forming at sub-micron scales [11] and building new materials [12].

Macroscopic crystal plasticity relies on a phenomenological continuum description of plastic deformation in terms of a finite number of order parameters representing amplitudes of pre-designed *mechanisms*. These mechanisms are coupled elastically and operate according to friction type dynamics [13–17]. The alternative microscopic approaches, relying instead on molecular dynamics [18–25], can handle only macroscopically insignificant time and length scales [26]. An intermediate discrete dislocation dynamics approach focuses on long range interaction of few dislocations, while their short range interaction is still treated phenomenologically [27–29]. Collective dynamics of many dislocations can be also described by the dislocation density field, however, rigorous coarse-graining in such strongly interacting system still remains a major challenge [30–37].

A highly successful computational bridge between microscopic and macroscopic approaches is provided by the quasi-continuum finite element method which uses adaptive meshing and employs ab initio approaches to guide the constitutive response at different mesh scales [38–42]. Its drawbacks, however, are spurious effects due to matching of FEM representations at different scales and a high computational cost of reconstructing the constitutive response at the smallest scales [43].

In this Letter we propose a synthetic approach dea-

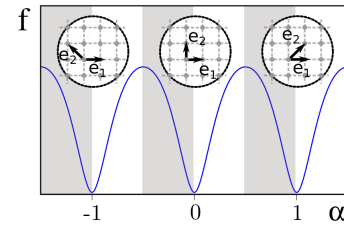


FIGURE 1. Schematic representation of a lattice invariant shear and the associated energy barriers along the simple shear loading path  $\nabla \mathbf{y} = \mathbb{1} + \alpha(\mathbf{e}_1 \otimes \mathbf{e}_1^\perp)$ . Alternating minimal periodicity domains are marked in gray and white.

ling with the macroscopic quantities such as stresses and strains, while accounting correctly for the exact symmetry of the crystal lattice. Our main assumption is that meso-scale material elements are exposed to the periodic energy landscape which resolves lattice-invariant strains, including shears related to slip [44, 45], see Fig. 1. Our approach follows the original proposal by Ericksen that the energy periodicity in the space of tensors should be made compatible with geometrically nonlinear kinematics of crystal lattices [46–49], and we also build upon subsequent important developments of the mathematical formalism in [50–54].

This general program can be viewed as far reaching generalization of the Frenkel-Kontorova-Peierls-Nabarro model accounting for energy periodicity along a single slip plane [55–57]. Scalar models with periodic energies, dealing with multiple slip planes, have been used before to describe dislocation cores [58–60], to simulate dislocation nucleation [61–64] and to capture intermittency of plastic flows [65, 66]. Their tensorial versions with *linearized* kinematics were considered in [67–70].

In the proposed kinematically *nonlinear* theory the role of the order parameter is played by the metric ten-

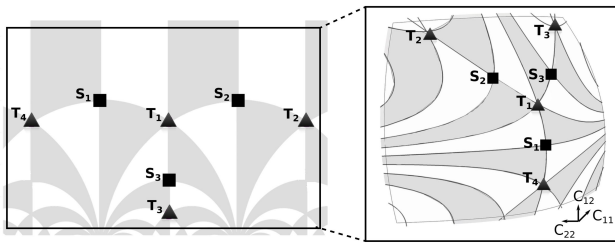


FIGURE 2. Structure of the  $GL(2, \mathbb{Z})$  periodicity domains in the space of metric tensors : (a) partition of the complex half-plane (Dedekind tessellation), (b) equivalent partition of the section  $\det \mathbf{C} = 1$  of the space  $\mathbf{C}$ . Points  $\mathbf{S}_i$  represent the same square lattice, points  $\mathbf{T}_i$  – the same triangular lattice.

sor (characterizing local deformation), and the bottoms of the energy wells correspond to lattice invariant deformations. The continuum Landau energy density of this type must be invariant under the infinite symmetry group  $GL(3, \mathbb{Z})$  and since the ground state in this case is necessarily hydrostatic [47, 71], the regularization is necessary. Theories incorporating various elements of the tensorial  $GL(3, \mathbb{Z})$  symmetry have already proved useful in the description of reconstructive phase transitions [72–77] and in this Letter we extend this idea to the modeling of crystal plasticity proper, see also [78].

From the perspective of Landau theory with an infinite number of *equivalent* energy wells, plastically deformed solid can be viewed as a multi-phase mixture of *equivalent* phases. Given the large magnitude of the ‘transformation strain’, such phases are localized at the scale of the regularizing length and the domain boundaries appear macroscopically as linear defects mimicking dislocations. Plastic yield can be then interpreted as an escape from the reference energy well and plastic mechanisms can be linked to low-barrier valleys in the energy landscape. Friction type dissipation emerges as a result of homogenization of an overdamped athermal dynamics in a rugged energy landscape [79, 80]. It is important to notice that such approach incorporates both long and short range dislocation interactions; it also correctly describes plastic slip even though the dislocations cores are regularized and blurred on the scale of the unit cell.

In this Letter we use this general approach to study the peculiarities of *collective* dislocation nucleation in crystals with different symmetries and show that in low symmetry lattices there is a nontrivial coupling between plastic mechanisms due to the presence of degenerate mountain passes representing lattices with higher symmetry. The crucial role in the formation of self induced plastic disorder is then played by the unstable high symmetry phases, traditionally thought to be unrelated to plastic flow. The general conclusion is that, rather paradoxically, the global crystal symmetry can induce frustration and become the cause of lattice incompatibility developing during plastic deformation.

Consider a continuous deformation  $\mathbf{y} = \mathbf{y}(\mathbf{x})$ , where  $\mathbf{y}$  are actual and  $\mathbf{x}$  are reference coordinates. The energy density of an elastic solid can depend on the deformation gradient  $\nabla \mathbf{y}$  only through the metric tensor  $\mathbf{C} = (\nabla \mathbf{y})^T \nabla \mathbf{y}$ . To account for all deformations that map a Bravais lattice into itself we must require that  $f(\mathbf{C}) = f(\mathbf{m}^T \mathbf{C} \mathbf{m})$  for any  $\mathbf{m}$  from a discrete group conjugate to  $GL(3, \mathbb{Z})$  and comprised of all invertible matrices with integral entries and determinant  $\pm 1$ , see Supplementary Material [81]. In the presence of such symmetry, the space of metric tensors  $\mathbf{C}$  partitions into *periodicity domains*, each one containing an energy well equivalent to the reference one. If we know the structure of the energy in one of such domains, we can use, for instance, the Lagrange reduction [54, 82] to find its value in any other point.

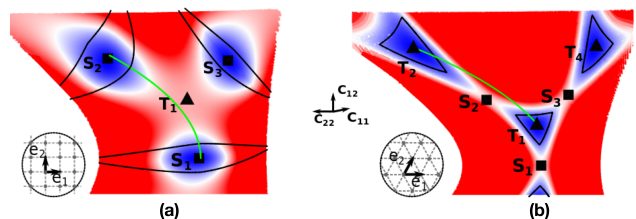


FIGURE 3. Energy landscapes corresponding to potential (1) with  $\beta = -1/4$  (a) and  $\beta = 4$  (b). Color indicate the energy level : blue-low, red-high. Black lines delimit the zones of linear stability for the homogeneous states. Green lines correspond to the simple shear loading paths discussed in the text.

In the special case of 2D lattices, which we focus on in what follows, a section  $\det \mathbf{C} = 1$  in the 3D space of tensors  $\mathbf{C}$  can be used to visualize the implied tensorial periodicity of the energy, see Fig 2. The global picture is made visible if we map this section into a complex half-plane using the function  $z = C_{11}^{-1}(C_{12} + i)$  [51, 52]. For instance, the point  $\mathbf{S}_1$  in Fig. 2, corresponding on the complex half plane to  $z = i$  describes a *square* lattice with the basis vectors aligned with the close-packed directions :  $\mathbf{e}_1 = (1, 0)$ ,  $\mathbf{e}_2 = (0, 1)$ . Simple shear  $\mathbb{1} + \mathbf{e}_1 \otimes \mathbf{e}_1^\perp$ , where  $\mathbf{e}_1^\perp$  is a vector orthogonal to  $\mathbf{e}_1$ , maps this point into its symmetric counterpart  $i + 1$  (point  $\mathbf{S}_2$ ); Another square lattice, corresponding to point  $\mathbf{S}_3$  in Fig. 2 with  $z = 1/2(1 + i)$ , can be obtained from the lattice  $\mathbf{S}_1$  by the shear  $\mathbb{1} + \mathbf{e}_2 \otimes \mathbf{e}_2^\perp$ . Instead, the point  $\mathbf{T}_1$  in Fig 2, corresponding to  $z = \frac{1}{2} + \frac{\sqrt{3}}{2}i$ , describes a *triangular* lattice (with hexagonal symmetry) whose basis vectors  $\mathbf{e}_1 = \gamma(1, 0)$ ,  $\mathbf{e}_2 = \gamma(1/2, \sqrt{3}/2)$  with  $\gamma = (4/3)^{1/4}$  are again aligned with the close-packed directions. Its closest equivalent neighbors are  $\mathbf{T}_2$  and  $\mathbf{T}_4$  corresponding to  $z = \frac{1}{2} + \frac{\sqrt{3}}{2}i \pm 1$ . They are reachable from  $\mathbf{T}_1$  by the shear deformation  $\mathbb{1} \pm \mathbf{e}_1 \otimes \mathbf{e}_1^\perp$ .

To demonstrate the possibility of yield-inducing instabilities in a material with such energy, it is sufficient to consider a system under the most constraining, af-

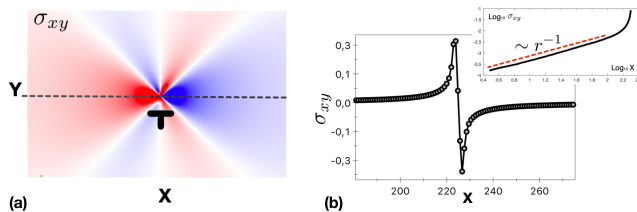


FIGURE 4. Single edge dislocation in a square lattice (interface between equivalent 'phases'  $\mathbf{S}_1$  and  $\mathbf{S}_2$ ); its Burgers vector is horizontal, with the length equal to the side of the square unit cell. (a) Finite element nodes with color indicating the level of Cauchy stress  $\sigma_{xy}$ ; (b) Stress profile along the glide plane; inset illustrates the far field asymptotics. System size  $1000 \times 1000$ .

fine displacement control. Given the gradient nature of the order parameter, the (spinodal) instability of a homogeneous state should be linked to the local loss of rank-one-convexity of the energy [83, 84]. This is equivalent to the loss of positive definiteness of the acoustic tensor  $\mathbf{Q}$  with components  $Q_{ik} = A_{ijkl}n_jn_l$ , where  $A_{ijkl} = \partial^2 f / (\partial_j y_i \partial_l y_k)$  is the fourth-order incremental elastic tensor and  $\mathbf{n}$  is a unit vector [85, 86].

For illustrative purposes we now choose a particular energy density  $f = f_v + f_d$  which decouples into a volumetric  $f_v(\det \mathbf{C})$  and a deviatoric  $f_d(\mathbf{C}/(\det \mathbf{C})^{1/2})$  parts. Since  $\det \mathbf{C}$  is invariant under  $\text{GL}(2, \mathbb{Z})$ , our symmetry constraints concern only the deviatoric part  $f_d$ . This function needs to be specified only inside a single periodicity domain with the suitable conditions on its boundary ensuring required smoothness [50]. The lowest order *polynomial* representation of  $f_d$ , which guarantees the continuity of the elastic moduli, was constructed in [54]; for the general non-polynomial representation see [51].

If the reference lattice is either square or triangular symmetry, the minimal potential can be chosen in the form [54] :

$$f_d(\tilde{\mathbf{C}}) = \beta \psi_1(\tilde{\mathbf{C}}) + \psi_2(\tilde{\mathbf{C}}) \quad (1)$$

where  $\psi_1 = I_1^4 I_2 - 41 I_2^3 / 99 + 7 I_1 I_2 I_3 / 66 + I_3^2 / 1056$ , and  $\psi_2 = 4 I_2^3 / 11 + I_1^3 I_3 - 8 I_1 I_2 I_3 / 11 + 17 I_3^2 / 528$ . The hexagonal invariants here have the structure :  $I_1 = \frac{1}{3}(\tilde{C}_{11} + \tilde{C}_{22} - \tilde{C}_{12})$ ,  $I_2 = \frac{1}{4}(\tilde{C}_{11} - \tilde{C}_{22})^2 + \frac{1}{12}(\tilde{C}_{11} + \tilde{C}_{22} - 4\tilde{C}_{12})^2$ , and  $I_3 = (\tilde{C}_{11} - \tilde{C}_{22})^2(\tilde{C}_{11} + \tilde{C}_{22} - 4\tilde{C}_{12}) - \frac{1}{9}(\tilde{C}_{11} + \tilde{C}_{22} - 4\tilde{C}_{12})^3$ . The choice  $\beta = -1/4$  enforces the square symmetry on the reference state, while choosing  $\beta = 4$  we bias the reference state towards hexagonal symmetry; the energy landscapes in those two cases are illustrated in Fig. 3. The volumetric energy density will be chosen in the simplest form  $f_v(s) = \mu(s - \log(s))$ , which excludes configurations with infinite compression; the coefficient  $\mu$  plays the role of a bulk modulus.

The resulting 'yield surfaces' are shown in Fig. 3. To understand the nature of the associated instabilities,

consider the case when a simple shear is imposed on the boundary

$$\nabla \mathbf{y} = \mathbf{1} + \alpha(\mathbf{e}_1 \otimes \mathbf{e}_1^\perp). \quad (2)$$

Starting, in the case of square lattice, from the homogeneous reference state  $\mathbf{S}_1$ , we find that at instability point the condition  $\det \mathbf{Q} = 0$  produces two, almost simultaneously destabilized directions  $\mathbf{q} = \nabla \mathbf{y}[\mathbf{n}] / |\nabla \mathbf{y}[\mathbf{n}]| = (\cos \xi, \sin \xi)$  : the first one with  $\xi \approx -0.11\text{rad}$ , almost perpendicular to the deformed  $\mathbf{e}_2$ , and the second one with  $\xi \approx 1.55\text{rad}$ , almost perpendicular to the deformed  $\mathbf{e}_1$ . The near-degeneracy of the bifurcation is an indicator that two 'slip planes' may be activated. In the case of triangular lattice, the instability along a similar loading path originating at  $\mathbf{T}_1$  produces a single unstable direction  $\xi \approx -1.25\text{rad}$  which is incommensurate with the lattice. In this case one can expect only one 'slip plane' to be activated. Our numerical experiments show that the acoustic-tensor-based analytical instability conditions are in agreement with direct numerical simulations.

Before addressing the post-bifurcational behavior consider a single edge dislocation trapped by the lattice somewhere far from the boundaries. In Fig. 4 we illustrate the corresponding stress distribution which matches the classical continuum far field with  $r^{-1}$  asymptotics while also resolving (at a scale of the mesh) the core region. Solutions like this can be helpful in calibrating the model using molecular statics simulations.

The collective nucleation pattern emerging after a stress drop is illustrated in Fig. 5 for both types of lattices. The results are presented on both, the configurational space, Fig. 5(a,c), where each point corresponds to a single element of the mesh and the actual physical space, Figs. 5(b,d), where the color of the dots (nodal points) indicate the level of stress. The configurational points, all located initially at the bottom of the reference energy well, disperse as a result of the massive nucleation event. The ensuing spatial dislocation distribution is quasi-regular with pile-ups at the rigid boundaries. Note the formation of characteristic entanglements with dislocations on two slip planes blocking each other (in the case of square lattice); there is also some disorder due to unavoidable numerical noise.

Note that in the case of square lattice, the system is driven by the loading device from the reference state  $\mathbf{S}_1$  towards the equivalent state  $\mathbf{S}_2$ . At the "yielding" threshold, which marks the end of the elastic regime, the homogeneous configuration  $\mathbf{S}_1$  loses stability and the ensuing pattern represents (outside the core regions) a mixture of three 'pure' states  $\mathbf{S}_1$ ,  $\mathbf{S}_2$  and  $\mathbf{S}_3$ , see Fig.5(a). While the appearance of the state  $\mathbf{S}_2$  is natural, because the corresponding 'plastic mechanism' is favored by the loading, the main complexity of the resulting dislocation pattern is due to the emergence of the state  $\mathbf{S}_3$ . It in-

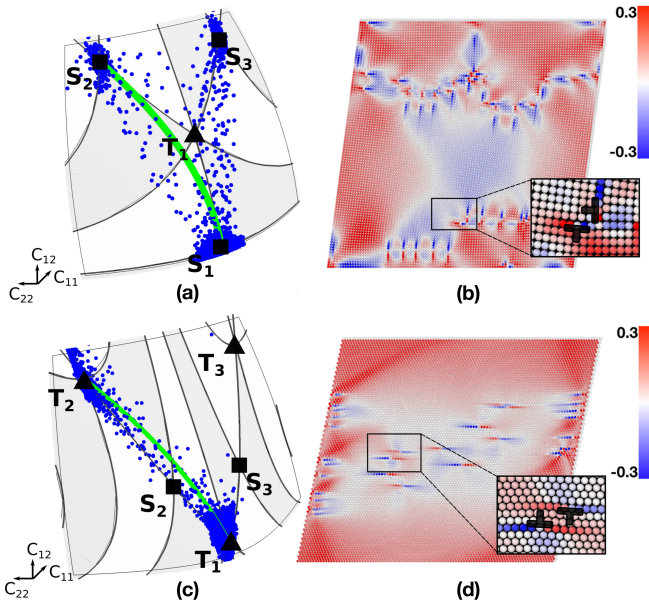


FIGURE 5. Collective dislocation nucleation : (a,b) square lattice, (c,d) triangular lattice. We show two representations of the same phenomenon : (a,c) in the configurational space, where green lines are simple shear paths imposed by the loading device and blue dots indicate the metric tensor distribution among the elements ; (b, d) in the physical space ; colors indicate the level of the nodal Cauchy stresses  $\sigma_{xy}$ . System size  $200 \times 200$ .

indicates the activation of the second plastic mechanism, decoupled (in the nonlinear theory) from the first one.

The appearance of the state  $\mathbf{S}_3$  can be understood if we recall that the linear stability analysis predicted two almost simultaneously unstable modes aligned with the slip directions in the deformed state. While one of these directions is indeed aiming towards the energy well  $\mathbf{S}_2$ , the other one, which bifurcates first, is directed towards  $\mathbf{S}_3$ . Our numerical simulations show that the latter instability mode grows faster which can be interpreted as, somewhat counter-intuitive, early stage dominance of the secondary 'plastic mechanism'. The flow of configurational points passes near the unstable equilibrium state  $\mathbf{T}_1$ , corresponding to a triangular lattice, where it splits into three streams directed towards the configurations  $\mathbf{S}_1$ ,  $\mathbf{S}_2$  and  $\mathbf{S}_3$ , see Movie S1 in [81].

This behavior becomes more transparent if we consider a smoother energy potential. Note that the symmetry transformations from  $GL(2, \mathbb{Z})$  correspond on the upper complex half-plane to the fractional (Moebius) transformations with integral entries of the type  $(m_{22}z + m_{12}) / (m_{21}z + m_{11})$  [50, 51]. This observation links the infinitely periodic energy densities for 2D crystalline materials with the classical modular functions [87], with the most well known example provided by the Klein invariant  $J(z)$  [88], see Supplementary Material for more details [81]. One can show that for this holomorphic function

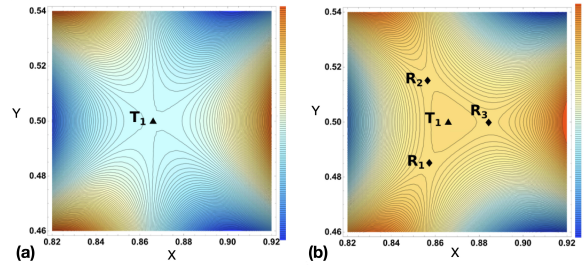


FIGURE 6. Level sets of the energy density on the surface  $\det \mathbf{C} = 1$  around the point  $\mathbf{T}_1$  : we use the parametrization  $C_{11} = 1/Y$ ,  $C_{22} = X^2 + Y^2/Y$ ,  $C_{12} = X/Y$  ; (a) Klein invariant based potential ; (b) polynomial potential (1) with  $\beta = -1/4$ .

$J|_{\mathbf{S}_i} = 1$ ,  $J'|_{\mathbf{S}_i} = 0$ , while  $J|_{\mathbf{T}_i} = J'|_{\mathbf{T}_i} = J''|_{\mathbf{T}_i} = 0$ . Therefore, the corresponding potentials with the reference square and triangular lattices can be chosen in the form :  $f_d(z) = |J(z) - 1|$  (square lattice) and  $f_d(z) = |J(z)|^{2/3}$  (triangular lattice) ; the exponents are chosen to ensure a non-degenerate linear-elastic response close to the bottoms of the energy wells. The energy landscapes and the yield surfaces for such potentials are qualitatively similar to the ones presented in Fig. 3.

Note that the choice  $f_d(z) = |J(z) - 1|$  for a square lattice turns the 'triangular' critical point  $\mathbf{T}_1$  and all its symmetric counterparts into degenerate 'monkey saddles', characterized by the local Taylor expansion of the form  $x^3 - 3xy^2$ , see Fig.6(a). The flow of configurational points directed initially towards such unstable state (say,  $\mathbf{T}_1$ ) will therefore necessarily split into three streams directed towards the stable states (say,  $\mathbf{S}_1$ ,  $\mathbf{S}_2$  and  $\mathbf{S}_3$ ).

Superficially, the situation looks a bit different in the case of the polynomial energy (1), where the Hessian is nondegenerate at the point  $\mathbf{T}_1$  which corresponds in this case to a shallow energy maximum. However this maximum is surrounded by the three nondegenerate saddles  $\mathbf{R}_1$ ,  $\mathbf{R}_2$  and  $\mathbf{R}_3$  describing rhombic lattices, see Fig.6(b), and the general conclusion about the activation of the secondary plastic mechanism and the ultimate dispersion over three energy wells  $\mathbf{S}_1$ ,  $\mathbf{S}_2$  and  $\mathbf{S}_3$  remains valid. Note that the implied coupling of the plastic mechanisms would have to be *postulated* in the phenomenological plasticity theory.

The picture is simpler in the case of a triangular lattice where the loading (2) from  $\mathbf{T}_1$  to  $\mathbf{T}_2$  produces a mixture of only two 'pure' states  $\mathbf{T}_1$ ,  $\mathbf{T}_2$ , see Fig.5(d). The latter can be interpreted as the activation of a single plastic mechanism, the one favored by the loading, see Movie S2 in [81].

To conclude, our model shows that crystal plasticity naturally arises from nonlinear elasticity, if the tensorial symmetry of the crystal lattice is properly accounted for. The memory of the atomic lattice in such infinitely periodic Landau theory is present in the form of the infor-

mation about the affine mappings that leave the energy density invariant. Athermal evolution in the regularized model of this type can lead to temporal and spatial complexity which our analysis predicts to be highly sensitive to both, the crystallographic symmetry and the orientation of the crystal [89, 90]. In particular, our study highlights the crucial role played in plastic deformation by the degenerate saddle points of the energy representing seemingly irrelevant, unstable crystallographic phases; for similar effects in other fields see [91–94]. More generally, the proposed Landau theory perspective on crystal plasticity promises to become an important new tool in the study of inelasticity at the micro/nano scales where the conventional engineering theories fail to access strength, account for fluctuations and adequately describe size effects [95–97].

---

\* Corresponding author: umut.salman@polytechnique.edu

- [1] D. Bonn, M. M. Denn, L. Berthier, T. Divoux, and S. Manneville, *Rev. Mod. Phys.* **89**, 035005 (2017).
- [2] A. H. Cottrell, in *Dislocations in Solids*, Vol. 11, edited by F. R. N. Nabarro and M. S. Duesbery (Elsevier, 2002) pp. vii–xvii.
- [3] W. Choi, Y. Chen, S. Papanikolaou, and J. Sethna, *Computing in Science & Engineering* **14**, 33 (2012).
- [4] A. Vinogradov and Y. Estrin, *Prog. Mater. Sci.* **95**, 172 (2018).
- [5] L. A. Zepeda-Ruiz, A. Stukowski, T. Oettel, and V. V. Bulatov, *Nature* **550**, 492 (2017).
- [6] O. Salman and L. Truskinovsky, *International Journal of Engineering Science* **59**, 219 (2012).
- [7] L. Kubin, *Dislocations, mesoscale simulations and plastic flow*, Vol. 5 (Oxford University Press, 2013).
- [8] P. D. Ispánovity, L. Laurson, M. Zaiser, I. Groma, S. Zapperi, and M. J. Alava, *Phys. Rev. Lett.* **112**, 235501 (2014).
- [9] D. A. Hughes and N. Hansen, *Acta Mater.* **148**, 374 (2018).
- [10] A. Irastorza-Landa, H. Van Swygenhoven, S. Van Petegem, N. Grilli, A. Bollhalder, S. Brandstetter, and D. Grolimund, *Acta Mater.* **112**, 184 (2016).
- [11] F. F. Csikor, C. Motz, D. Weygand, M. Zaiser, and S. Zapperi, *Science* **318**, 251 (2007).
- [12] D. L. McDowell, in *Computational Materials System Design*, edited by D. Shin and J. Saal (Springer International Publishing, Cham, 2018) pp. 105–146.
- [13] F. Roters, P. Eisenlohr, L. Hantcherli, D. D. Tjahjanto, T. R. Bieler, and D. Raabe, *Acta Mater.* **58**, 1152 (2010).
- [14] S. Forest, J. R. Mayeur, and D. L. McDowell, “Micromorphic crystal plasticity,” in *Handbook of Nonlocal Continuum Mechanics for Materials and Structures*, edited by G. Z. Voyiadjis (Springer International Publishing, Cham, 2019) pp. 643–686.
- [15] M. E. Gurtin and L. Anand, *J. Mech. Phys. Solids* **57**, 405 (2009).
- [16] C. S. Han, H. Gao, Y. Huang, and W. D. Nix, *J. Mech. Phys. Solids* **53**, 1188 (2005).
- [17] in *Encyclopedia of Computational Mechanics Second Edition*, CISM Courses and Lectures No. 292, Vol. 44, edited by E. Stein, R. de Borst, and T. J. R. Hughes (John Wiley & Sons, Ltd, Chichester, UK, 2018) pp. 1–23.
- [18] Y.-M. Juan and E. Kaxiras, *Journal of Computer-Aided Materials Design* **1**, 55 (1993).
- [19] V. Bulatov, F. F. Abraham, L. Kubin, B. Devincere, and S. Yip, *Nature* **391**, 669 (1998).
- [20] D. Lyu and S. Li, *J. Mech. Phys. Solids* **122**, 613 (2019).
- [21] D. L. McDowell, “Connecting lower and higher scales in crystal plasticity modeling,” in *Handbook of Materials Modeling : Methods: Theory and Modeling*, edited by W. Andreoni and S. Yip (Springer International Publishing, Cham, 2018) pp. 1–21.
- [22] P. Moretti, B. Cerruti, and M.-C. Miguel, *PLoS One* **6**, e20418 (2011).
- [23] A. Skaugen, L. Angheluta, and J. Viñals, *Phys. Rev. Lett.* **121**, 255501 (2018).
- [24] J. M. Tarp, L. Angheluta, J. Mathiesen, and N. Goldenfeld, *Phys. Rev. Lett.* **113**, 265503 (2014).
- [25] K. R. Elder, M. Katakowski, M. Haataja, and M. Grant, *Phys. Rev. Lett.* **88**, 245701 (2002).
- [26] D. L. McDowell, in *Mesoscale Models : From Micro-Physics to Macro-Interpretation*, edited by S. Mesarovic, S. Forest, and H. Zbib (Springer International Publishing, Cham, 2019) pp. 195–297.
- [27] L. E. Shilkrot, R. E. Miller, and W. A. Curtin, *J. Mech. Phys. Solids* **52**, 755 (2004).
- [28] H. Song, H. Yavas, E. V. d. Giessen, and S. Papanikolaou, *J. Mech. Phys. Solids* **123**, 332 (2019).
- [29] J. A. El-Awady, H. Fan, and A. M. Hussein, in *Multiscale Materials Modeling for Nanomechanics*, Vol. 245 (2016) p. 337.
- [30] A. El-Azab, *Phys. Rev. B Condens. Matter* **61**, 11956 (2000).
- [31] S. Xia and A. El-Azab, *Modell. Simul. Mater. Sci. Eng.* **23**, 055009 (2015).
- [32] I. Groma, in *Mesoscale Models : From Micro-Physics to Macro-Interpretation*, edited by S. Mesarovic, S. Forest, and H. Zbib (Springer International Publishing, Cham, 2019) pp. 87–139.
- [33] A. Acharya and A. Roy, *J. Mech. Phys. Solids* **54**, 1687 (2006).
- [34] Y. S. Chen, W. Choi, S. Papanikolaou, M. Bierbaum, and J. P. Sethna, *Int. J. Plast.* **46**, 94 (2013).
- [35] S. Sandfeld, T. Hochrainer, M. Zaiser, and P. Gumbsch, *J. Mater. Res.* **26**, 623 (2011).
- [36] R. LeSar, *Annu. Rev. Condens. Matter Phys.* **5**, 375 (2014).
- [37] P.-L. Valdenaire, Y. Le Bouar, B. Appolaire, and A. Finel, *Phys. Rev. B Condens. Matter* **93**, 214111 (2016).
- [38] E. B. Tadmor, M. Ortiz, and R. Phillips, *Philos. Mag. A* **73**, 1529 (1996).
- [39] E. B. Tadmor and R. E. Miller, *Modell. Simul. Mater. Sci. Eng.* **25**, 071001 (2017).
- [40] D. M. Kochmann and J. S. Amelang, in *Multiscale Materials Modeling for Nanomechanics*, edited by C. R. Weinberger and G. J. Tucker (Springer International Publishing, Cham, 2016) pp. 159–193.
- [41] J. Li, K. J. Van Vliet, T. Zhu, S. Yip, and S. Suresh, *Nature* **418**, 307 (2002).
- [42] J. Li, T. Zhu, S. Yip, K. J. Van Vliet, and S. Suresh, *Materials Science and Engineering : A* **365**, 25 (2004).
- [43] M. Luskin and C. Ortner, *Acta Numer.* **22**, 397 (2013).
- [44] V. Bulatov and A. Argon, *Modelling and Simulation in*

- Materials Science and Engineering **2**, 167 (1994).
- [45] E. Kaxiras and L. Boyer, *Physical Review B* **50**, 1535 (1994).
- [46] J. L. Ericksen, *Int. J. Solids Struct.* **6**, 951 (1970).
- [47] J. L. Ericksen, in *Nonlinear Elasticity*, edited by R. W. Dickey (Academic Press, 1973) pp. 161–173.
- [48] J. L. Ericksen, in *Advances in Applied Mechanics*, Vol. 17, edited by C.-S. Yih (Elsevier, 1977) pp. 189–244.
- [49] J. L. Ericksen, *Arch. Ration. Mech. Anal.* **73**, 99 (1980).
- [50] G. P. Parry, *Math. Proc. Cambridge Philos. Soc.* **80**, 189 (1976).
- [51] I. Folkins, *J. Math. Phys.* **32**, 1965 (1991).
- [52] G. P. Parry, *Arch. Ration. Mech. Anal.* **145**, 1 (1998).
- [53] M. Pitteri and G. Zanzotto, *Continuum models for phase transitions and twinning in crystals* (Chapman and Hall/CRC, 2002).
- [54] S. Conti and G. Zanzotto, *Arch. Ration. Mech. Anal.* **173**, 69 (2004).
- [55] J. Frenkel and T. Kontorova, *Izv. Akad. Nauk, Ser. Fiz.* **1**, 137 (1939).
- [56] R. Peierls, *Proc. Phys. Soc. London* **52**, 34 (1940).
- [57] F. R. N. Nabarro, *Proc. Phys. Soc. London* **59**, 256 (1947).
- [58] A. S. Kovalev, A. D. Kondratyuk, A. M. Kosevich, and A. I. Landau, *phys. stat. sol. (b)* **177**, 117 (1993).
- [59] A. I. Landau, *phys. stat. sol. (b)* **183**, 407 (1994).
- [60] A. Carpio and L. L. Bonilla, *Phys. Rev. Lett.* **90**, 135502 (2003).
- [61] I. Plans, A. Carpio, and L. L. Bonilla, *EPL* **81**, 36001 (2007).
- [62] L. L. Bonilla, A. Carpio, and I. Plans, *Physica A : Statistical Mechanics and its Applications* **376**, 361 (2007).
- [63] P. Lomdahl and D. Srolovitz, *Phys. Rev. Lett.* **57**, 2702 (1986).
- [64] D. Srolovitz and P. Lomdahl, *Physica D : Nonlinear Phenomena* **23**, 402 (1986).
- [65] O. U. Salman and L. Truskinovsky, *Phys. Rev. Lett.* **106**, 175503 (2011).
- [66] O. U. Salman and L. Truskinovsky, *Int. J. Eng. Sci.* (2012).
- [67] A. Minami and A. Onuki, *Acta Mater.* **55**, 2375 (2007).
- [68] A. Onuki, *Phys. Rev. E Stat. Nonlin. Soft Matter Phys.* **68**, 061502 (2003).
- [69] A. Carpio and L. L. Bonilla, *Phys. Rev. B Condens. Matter* **71**, 134105 (2005).
- [70] P.-A. Geslin, B. Appolaire, and A. Finel, *Acta Mater.* **71**, 80 (2014).
- [71] I. Fonseca, *Arch. Ration. Mech. Anal.* **97**, 189 (1987).
- [72] V. P. Dmitriev, S. B. Rochal, Y. M. Gufan, and P. Tolledano, *Phys. Rev. Lett.* **60**, 1958 (1988).
- [73] B. Horovitz, R. J. Gooding, and J. A. Krumhansl, *Phys. Rev. Lett.* **62**, 843 (1989).
- [74] M. Sanati, A. Saxena, T. Lookman, and R. C. Albers, *Phys. Rev. B Condens. Matter* **63**, 224114 (2001).
- [75] K. Bhattacharya, S. Conti, G. Zanzotto, and J. Zimmer, *Nature* **428**, 55 (2004).
- [76] F. J. Pérez-Reche, L. Truskinovsky, and G. Zanzotto, *Continuum Mech. Thermodyn.* **21**, 17 (2009).
- [77] A. Vattré and C. Denoual, *J. Mech. Phys. Solids* **92**, 1 (2016).
- [78] P. Biscari, M. F. Urbano, A. Zanzottera, and G. Zanzotto, *J. Elast.* **123**, 85 (2015).
- [79] G. Puglisi and L. Truskinovsky, *J. Mech. Phys. Solids* **53**, 655 (2005).
- [80] A. Mielke and L. Truskinovsky, *Arch. Ration. Mech. Anal.* **203**, 577 (2011).
- [81] See Supplemental Material at [URL will be inserted by publisher] for the details on the energy invariance, mapping of the configurational space into the upper complex plane, computation of the Klein invariant, the numerical implementation of the model and for the description of the supplementary Movie 1 and Movie 2.
- [82] P. Engel, *Geometric Crystallography : An Axiomatic Introduction to Crystallography* (Springer Netherlands, 1986).
- [83] R. Ogden, “Non-linear elastic deformations. ellis horwood, chichester 1984.” (1997).
- [84] Y. Grabovsky and L. Truskinovsky, *J. Nonlinear Sci.* **24**, 1125 (2014).
- [85] K. J. Van Vliet, J. Li, T. Zhu, S. Yip, and S. Suresh, *Phys. Rev. B Condens. Matter* **67**, 104105 (2003).
- [86] R. E. Miller and D. Rodney, *J. Mech. Phys. Solids* **56**, 1203 (2008).
- [87] B. Schoeneberg, *Elliptic modular functions : an introduction*, Vol. 203 (Springer Science & Business Media, 2012).
- [88] A. van Wijngaarden, in *Indagationes Mathematicae (Proceedings)*, Vol. 56 (Elsevier, 1953) pp. 389–400.
- [89] J. Weiss, W. B. Rhouma, T. Richeton, S. Dechanel, F. Louchet, and L. Truskinovsky, *Phys. Rev. Lett.* **114**, 105504 (2015).
- [90] G. Sparks and R. Maaß, *Phys. Rev. Materials* **2**, 120601 (2018).
- [91] J. Rehbein and B. K. Carpenter, *Physical Chemistry Chemical Physics* **13**, 20906 (2011).
- [92] D. Wales, *Energy landscapes : Applications to clusters, biomolecules and glasses* (Cambridge University Press, 2003).
- [93] A. Shtyk, G. Goldstein, and C. Chamon, *Physical Review B* **95**, 035137 (2017).
- [94] F. Bociort and M. van Turnhout, in *Optical Design and Engineering II*, Vol. 5962 (International Society for Optics and Photonics, 2005) p. 59620S.
- [95] J. R. Greer and J. T. M. De Hosson, *Progress in Materials Science* **56**, 654 (2011).
- [96] H. Zhang, J. Tersoff, S. Xu, H. Chen, Q. Zhang, K. Zhang, Y. Yang, C.-S. Lee, K.-N. Tu, J. Li, *et al.*, *Science advances* **2**, e1501382 (2016).
- [97] P. Zhang, O. U. Salman, J.-Y. Zhang, G. Liu, J. Weiss, L. Truskinovsky, and J. Sun, *Acta Materialia* **128**, 351 (2017).